HHS Public Access

Author manuscript

Biochem J. Author manuscript; available in PMC 2017 October 01.

Published in final edited form as:

Biochem J. 2016 October 01; 473(19): 3049–3063. doi:10.1042/BCJ20160537.

Structural basis of arginine asymmetrical dimethylation by PRMT6

Hong Wu[1], **Weihong Zheng**[2], **Mohammad S. Eram**[1], **Mynol Vhuiyan**[3], **Aiping Dong**[1], **Hong Zeng**[1], **Hao He**[1], **Peter Brown**[1], **Adam Frankel**[3], **Masoud Vedadi**[1,4], **Minkui Luo**[2], and **Jinrong Min**[1,5,*]

[1]Structural Genomics Consortium, University of Toronto, Toronto, Ontario M5J 1L7, Canada

[2]Chemical Biology Program, Memorial Sloan-Kettering Cancer Center, New York, NY 10065, USA

[3]Faculty of Pharmaceutical Sciences, The University of British Columbia, 2405 Wesbrook Mall, Vancouver, BC V6T 1Z3, Canada

[4]Department of Pharmacology and Toxicology, University of Toronto; 1 King's College Circle, Toronto, Ontario, Canada, M5S 1A8

[5]Department of Physiology, University of Toronto, Toronto, Ontario M5S 1A8, Canada

Abstract

PRMT6 is a type I protein arginine methyltransferase, generating the asymmetric dimethylarginine mark on proteins such as histone H3R2. Asymmetric dimethylation of histone H3R2 by PRMT6 acts as a repressive mark that antagonizes trimethylation of H3 lysine 4 by the MLL histone H3K4 methyltransferase. PRMT6 is overexpressed in several cancer types, including prostate, bladder and lung cancers; therefore, it is of great interest to develop potent and selective inhibitors for PRMT6. Here we report the synthesis of a potent bi-substrate inhibitor GMS (6′-methyleneamine sinefungin, an analogue of sinefungin), and the crystal structures of human PRMT6 in complex respectively with SAH and the bi-substrate inhibitor GMS that shed light on the significantly improved inhibition effect of GMS on methylation activity of PRMT6 compared to SAH and a SAM competitive methyltransferase inhibitor sinefungin (SNF). In addition, we also crystallized PRMT6 in complex with SAH and a short arginine containing peptide. Based on the structural information here and available in the PDB database, we propose a mechanism that can rationalize the distinctive arginine methylation product specificity of different types of arginine methyltransferases and pinpoint the structural determinant of such a specificity.

Introduction

Arginine methylation is an abundant covalent post-translational modification. In two separate accounts, it was reported that about 2% of arginine residues in the total protein extracts from rat liver nuclei [1], and over 10% of proteins encoded in the *T. brucei* genome

*Correspondence should be addressed to J.M. (jr.min@utoronto.ca).

Conflict of interest statement

None declared.

are arginine methylated [2]. Arginine methylation exists in three forms, *i.e.*, mono-methylation (Rme1), asymmetric di-methylation (Rme2a) and symmetric di-methylation (Rme2s), which are carried out by three different types of protein arginine methyltransferases (PRMTs). PRMT1, 2, 3, 4, 6, and 8 (type I PRMT) generate asymmetric di-methylarginine modifications, PRMT5 and 9 (type II PRMT) generate symmetric di-methylarginine modifications, and PRMT7 (type III) is an arginine mono-methyltransferase [3, 4]. Arginine methylation is involved in a variety of cellular processes, such as transcriptional regulation, RNA processing, signal transduction, DNA repair and genomic stability [5].

Arginine methylation executes its functions normally through regulating protein-protein interactions either positively or negatively. For instance, the PRMT5-containing methylosome modifies some specific arginine sites to symmetric di-methylation in several spliceosomal Sm proteins, which are recognized by the Tudor domain of the SMN protein [6–8]. The SMN complex binds both arginine-methylated Sm proteins and snRNAs, bringing them together and facilitating Sm core assembly [9]. The same PRMT5-containing methyltransferase complex also methylates the Piwi proteins (PIWIL1-4), which contain multiple arginine-glycine (RG) and arginine-alanine (RA) repeats at their N-termini. Methylation of the Piwi proteins is required for their interaction with the TDRD group of germline-enriched Tudor domain proteins, such as TDRD1, TDRD2, TDRD4-9 and TDRD12, which leads to subsequent localization of these proteins to the meiotic nuage [10–13]. CARM1 (PRMT4) is a transcriptional coactivator that asymmetrically dimethylates histone H3R17. The histone H3R17me2a mark is recognized by the Tudor domain of TDRD3, consistent with the observation that TDRD3 is recruited to an estrogen-responsive element in a CARM1-dependent manner and promotes transcription by binding methyl-arginine marks on histone tails [8, 14]. PRMT6 is a histone H3R2 methyltransferase. Asymmetric dimethylation of histone H3R2 by PRMT6 acts as a repressive mark that antagonizes trimethylation of H3 lysine 4 by the MLL histone H3K4 methyltransferase [15–18]. Asymmetric dimethylation of histone H3R2 diminishes its binding to WDR5 and impedes the recruitment of WDR5 to euchromatic regions [19, 20]. WDR5 is a common component of the SET1/MLL family of histone H3K4 methyltransferases, and has been shown to bind different arginine containing peptides, including histone H3R2 [20–24]. Strikingly, when histone H3R2 is symmetrically dimethylated (H3R2me2s) by PRMT5, its binding to WDR5 is enhanced and the target genes are poised for transcriptional activation [19].

PRMT6 has been shown to modify histone H3R2 and a few other substrates, and it was reported recently that PRMT6 is overexpressed in several cancer types, and knockdown of PRMT6 significantly suppresses growth of bladder and lung cancer cells [25]. It was further shown that the tumor suppressor genes p21 and p27, two members of the CIP/KIP family of cyclin-dependent kinase (CDK) inhibitors, are direct targets of PRMT6 by methylating histone H3R2 in their promoters. Knockdown of PRMT6 leads to up-regulation of p21 and p27 and cellular senescence [26–28]. Hence, PRMT6 promotes cell growth and prevents senescence, making it an attractive therapeutic target for various types of cancer. In addition, PRMT6 is also implicated in the regulation of gene expression of TSP-1, a potent natural inhibitor of angiogenesis [29, 30], and the RUNX1 target genes, a group of genes implicated

in differentiation of hematopoietic stem/progenitor cells [31], and genes involved in maintaining embryonic stem cell identity [32]. PRMT6 also acts as a restriction factor for viral replication in human immunodeficiency virus pathogenesis by methylating TAT and other HIV proteins [33].

So far, crystal structures for several arginine methyltransferases have been determined, but it is still unclear how different types of arginine methyltransferases achieve the distinctive arginine methylation product specificity. In addition, considering the importance of PRMT6 in gene regulation and its dysregulation implicated in many different cancers, it is of great interest to develop potent inhibitors for PRMT6. In this study, we synthesized a potent bi-substrate inhibitor GMS for PRMT6, obtained its crystal structure in complex with PRMT6, and demonstrated that GMS exhibits better inhibition than sinefungin (SNF), a natural SAM (*S*-adenosyl-*L*-methionine) analog and potent inhibitor of methyltransferases. Furthermore, we crystallized PRMT6 in complex with SAH and a short peptide of a sequence GR(me1)G. By comparing these structures to those available crystal structures of other arginine methyltransferases, we are able to explain why different types of arginine methyltransferases generate the distinctive arginine methylation products specificity.

Materials and Methods

Cloning, expression and purification

A DNA fragment encoding full-length human PRMT6 (residues 1–375) was cloned into a baculovirus expression vector pFBOH-MHL (http://www.thesgc.org/sites/default/files/toronto_vectors/pFBOH-MHL.pdf). The protein was expressed in Sf9 cells (Invitrogen) with addition of 18 amino acid residues including a hexa-His tag followed by a TEV cleavage site (MHHHHHHSSGRENLYFQG) at the N-terminus. The harvested cells were resuspended in lysis buffer containing 20 mM Tris-HCl, pH 8.0, 500 mM NaCl, 5 mM imidazole, 2 mM β-mercaptoethanol, 5% glycerol, 0.6% NP-40, protease inhibitor cocktail (Roche), 3000 U of benzonase (Novagen). Cells were lysed by brief sonication. The clarified lysate was loaded onto a 2-mL TALON column (Clonetech). The column was washed with 50 column volumes of 20 mM Tris-HCl buffer, pH 8.0, containing 500 mM NaCl, 5% glycerol and 5 mM imidazole. The bound protein was eluted with elution buffer containing 20 mM Tris-HCl, pH 8.0, 500 mM NaCl, 5% glycerol and 250 mM imidazole. The eluted protein was loaded onto a Superdex200 column (GE Healthcare), equilibrated with 20 mM Tris-HCl buffer, pH 8.0 and 150 mM NaCl. Pooled fractions containing PRMT6 were subjected to TEV treatment to remove the His-tag. The protein was further purified to homogeneity by ion-exchange chromatography.

Inhibition assay

A scintillation proximity assay (SPA) method was used to determine the activity of PRMT6 as described previously [34, 35]. In brief, the reaction mixture (20 μL volume) was composed of 20 mM bis-tris-propane (pH 7.5), 0.01% Tween-20, 0.5% DMSO, 10 mM DTT, 50 nM PRMT6, 0.6 μM biotinylated H4(1–24) peptide (Tufts University Peptide Synthesis Core Facility, Boston, Ma). To start the reaction SAM was added at final concentration of 2.3 μM which include 57% ^{3}H-SAM (PerkinElmer Life Sciences,

cat#NET155V001MC; specific activity range 12–18 Ci/mmol) and 43% SAM (AK Scientific, Union City, CA). Due to highly acidic nature of the ^{3}H-SAM solution, non-tritiated (cold) SAM was used to supplement the reactions when necessary. For IC_{50} determination, different concentrations of compounds were added to the reaction mixture. The reactions were started by adding the substrate. Reaction mixtures were incubated at 23 °C for 20 minutes and were quenched by addition of 20 μL of 7.5 M guanidinium hydrochloride (GuHCl) followed by the addition of 180 μL of 20 mM Tris-HCl, pH 8.0. The quenched reactions were then transferred to the wells of a streptavidin and scintillant-coated microplate (FlashPlate® PLUS; PerkinElmer Life Sciences). The amount of the methylated peptide was quantified by tracing the radioactivity (CPM; counts per minute) as measured by a TopCount NXT™ Microplate Scintillation Counter (PerkinElmer Life Sciences). The IC_{50} values were calculated using SigmaPlot® software (SYSTAT Software Inc., CA, USA). To determine the optimal pH, the reactions (with no compound) were carried out in bis-tris-propane (20 mM) at pH values between 6–9.5 (Supplementary Fig. 4). The potency of the compounds were determined against PRMT1, PRMT3, CARM1 (PRMT4), PRMT5, PRMT6, and PRMT8 as well as few lysine methyltransferases (DOT1L, G9a, SETD7, and PRDM9) using a radioactivity based method, as described previously [34, 36, 37].

Methylarginine quantitation

The reactions were run overnight at 23 °C in a reaction mixture containing 20 mM bis-tris-propane (pH 7.5), 0.01% Tween-20, 0.5% DMSO, 10 mM DTT, 1 μM PRMT6, 8 μM peptide, and 5 μM of ^{3}H-SAM (Perkin Elmer Life Sciences, specific activity range 12–18 Ci/mmol). The samples were spin-filtered at 14,000 *g* at 4 °C using 10-kDa molecular weight cut-off filters (Nanosep, OD010C34) for 15 min to separate the enzyme from the peptide substrate. Sample eluates were transferred into 300 μL glass tubes and dried using a Thermo Savant SC110A speed vacuum. The dried reactions were hydrolyzed with 200 μL 6 N HCl at 110 °C for 24 h *in vacuo*. The dried samples were reconstituted in 100 μL of 0.5% acetic acid and 0.01% trifluoroacetic acid (TFA) mixture. The samples were quantified by LC-MS/MS with previously described buffer conditions and multiple reaction monitoring protocols [38].

Crystallization

Purified PRMT6 (5 mg/mL) was incubated with SAH (*S*-adenosyl-*L*-homocysteine, Sigma), GSM and SAH/peptide at 1:5 molar ratio of protein:ligand and crystallized using the hanging drop vapor diffusion method at 20 °C by mixing 1 μL of the protein solution with 1 μL of the reservoir solution. The complex crystals were obtained in solution containing 15% PEG 3350, 0.1 M succinate acid, pH 7.0 for PRMT6-SAH, 25% PEG 3350, 0.2 M KSCN for PRMT6-GSM and 10% PEG 8000, 0.1 M Tris-HCl, pH 8.5 for PRMT6-SAH-GR(me)G peptide, respectively.

Data Collection and Structure Determination

X-ray diffraction data for PRMT6-SAH, PRMT6-GMS and PRMT6-SAH-GR(me)G peptide complexes were collected at 100K at beam line 19ID-D of Advanced Photon Source (APS), Argonne National Laboratory. Data sets were processed using the HKL-3000 suite [39]. All the structures were solved by molecular replacement using MOLREP [40] with PDB entry

1G6Q as the search template. REFMAC [41] was used for structure refinement. The graphics program COOT [42] was used for model building and visualization. Molprobity [43] was used for structure validation.

Results and Discussion

Crystal structure of PRMT6 in complex with SAH

The crystal structure of full-length human PRMT6 in complex with SAH has been determined at a resolution of 1.97 Å (Fig. 1). The detailed crystal diffraction data and refinement statistics are summarized in Table 1. In this high-resolution crystal structure, the N-terminal 47 residues of PRMT6 are not visible. Although all the PRMT proteins share a conserved catalytic domain (Fig. 2), they have a variable N-terminal fragment that has been proposed to regulate methyl transfer activity and substrate specificity [44]. Consistently, the N-terminal fragment of PRMT6 has been reported to be necessary and sufficient for its association with other binding partners and plays a role in substrate specificity [45].

Similar to other solved type I PRMT structures, including PRMT1 [46, 47], PRMT3 [48, 49], CARM1/PRMT4 [50, 51], mouse PRMT6 [52] and *Trypanosoma brucei* PRMT6 (*Tb*PRMT6) [53], the catalytic domain of human PRMT6 consists of two domains, *i.e.*, the N-terminal Rossmann fold, and the C-terminal β-barrel domain with a dimerization arm embedded within it (Fig. 1). Like other type I PRMT proteins, PRMT6 also exists as a dimer, with the dimerization arm (helixes α4–6, colored in green) from one monomer packing against helixes αY/Z and α1/2 of the Rossmann domain from the other monomer to form a ring-like dimer architecture (Fig. 1B). The SAH molecule is bound in an extended conformation in a pocket formed by the Rossmann fold domain (Fig. 1B and 3A). The adenine ring, ribose moiety and homocysteine carboxylate of SAH are bound by PRMT6 through a series of hydrogen bonds and salt bridges, which are highly conserved in the PRMT family (Fig. 2 and 3A).

Structural comparisons of PRMT6 to the other type I enzymes reveals two interesting structural features of PRMT6 (Fig. 3C). First, the conserved Y(F/Y)xxY motif in the N-terminus of the Rossmann fold domain points away from the SAH binding pocket. This motif for CARM1 is disordered in the absence of SAH, but becomes an ordered helix and acts as a lid to cover the adenosine part of SAH in the CARM1-SAH binary complex (Fig. 3B and 3C). As a result, the SAH molecule is almost completely buried with the methyl group of the methyl donor cofactor SAM being only accessible to the substrate arginine via a narrow opening in the active site (Fig. 3D, PDB: 3B3F) [51]. The same phenomenon was also observed in the SAH-free and SAH bound PRMT3 structures [45, 49]. On the other hand, this motif in PRMT1 was found to be disordered or point away from SAH in either the presence or absence of SAH [46, 47], which leaves the SAH molecule widely exposed to the solvent, similar to what we have observed in the PRMT6-SAH structure (Fig. 3E). It has been shown previously that Y(F/Y)xxY plays an important role in SAH binding and catalysis in PRMT1, because deletion of this motif diminishes SAH binding and abolishes enzymatic activity [47]. Hence, we believe that this aromatic residue rich motif in the highly conserved catalytic domain of the type I PRMT proteins would adopt different conformations to open and close the SAH binding site to allow exit of SAH during catalysis.

Second, although all the type I PRMT proteins have a dimerization arm, structural alignment of all the available PRMT structures reveal that the dimerization arm in PRMT6 has a different conformation, which in turn leads to a flat dimer ring structure with a wide central cavity, whereas the two monomers in the PRMT1, PRMT3 and CARM1 dimers form a concave surface (Supplementary Fig. 1). The substrates access the active site of methyl transfer through the central cavity and the size and shape of the substrate binding groove determines the substrate specificity of different PRMTs [51, 54]; therefore, the unique dimer ring structure of PRMT6 may be a structural determinant for its substrate preference.

Synthesis of a bi-substrate compound as a potent PRMT6 inhibitor

The crystal structures of PRMT6 and other PRMTs in complex with SAH or sinefungin further inspired us to develop sinefungin analogues containing the features of substrates as bi-substrate inhibitors of PRMTs, such as 6′-methyleneamine sinefungin (GMS, **1**), which was synthesized from a known oxazolidinone imide precursor **2** [55] (Fig. 4A). The reduction of the chiral auxiliary imide of **2** led to the primary alcohol **3** with the desired steric center maintained at the C6 position of D-ribose ring. The approach was then implemented to introduce the amine functionality via **4** by Dess-Martin oxidation of the primary alcohol **3** and then reductive amination with benzyl amine, followed by carbobenzyloxy (Cbz) protection. The terminal alkene of the intermediate **4** was readily converted into the protected amino acid **5** as described previously [56]. After acidic cleavage of dihydropyrazine and *N*-trifuoroacetylation (TFA), the protecting groups on glycoside were exchanged with acetyl to facilitate the following adenosylation. The β-ribosyl adenine in **6** was installed through Vorbrüggen glycosylation of bis-silyl-*N*-benzoyladenine [56]. Here the amino acid in **6** was masked with *N*-trifuoroacetyl group rather than the previously-reported Cbz or acetyl group [57] for its orthogonality to hydrogenolysis and ease of removal. The hydrogenolysis condition set the primary amine on 6′ position free for further guanidylation. Trifluoroethanol was used as solvent to avoid *N*-alkylation in alcoholic solvent [58]. At last, global deprotection of base-labile blocking groups in the present of lithium hydroxide, followed by acidic removal of *t*-butoxycarbonyl completed the synthesis of the target compound GMS (Refer to the Supporting Methods for the detailed synthesis method).

We then applied the scintillation proximity assay (SPA) method to determine the inhibition activity of this compound against PRMT6, which showed an inhibition IC_{50} of 90 nM. That is significantly more potent than the SAM reaction product SAH and the SAH analog sinefungin (Fig. 4B). We also determined the specificity of GMS over other PRMTs and some selected lysine methyltransferases (Supplementary table 1). These data indicated that GMS preferentially inhabited some type 1 PRMTs, such as PRMT6, PRMT8 and CRAM1 (Supplementary table 1).

Crystal structure of PRMT6 in complex with the bi-substrate inhibitor GMS

In order to understand the enhanced inhibition effect of GMS against PRMT6, we have determined the crystal structure of PRMT6 in complex with the bi-substrate inhibitor GMS at a resolution of 1.88 Å (Fig. 5A). The PRMT6-GMS binary structure is almost identical to that of the PRMT6-SAH complex, and the Cα of these two structures can be superimposed

with a RMSD of just 0.25 Å. When these two complex structures are overlaid together, the SAH molecule in the PRMT6-SAH structure can perfectly superimpose with the corresponding moiety of the GMS molecule in the PRMT6-GMS complex structure. All the interactions between PRMT6 and SAH in the PRMT6-SAH binary structure are conserved in the GMS complex structure. However, GMS makes two extra hydrogen bonds through its guanidino moiety with PRMT6 (Fig. 5A). Namely, the terminal guanidino nitrogen atom in the guanidino moiety forms hydrogen bonds with the side chain carboxylate oxygen of E155 and the main chain carbonyl oxygen of M157, respectively (Fig. 5A). The extra interactions between GMS and PRMT6 presumably account for the significantly improved inhibition effect of GMS on the methylation activity of PRMT6, compared to SNF and SAH. When we superimposed the PRMT6-GMS complex structure with the PRMT1 ternary complex structure (PDB code: 1OR8 [47]), we found that the SAH molecule in the PRMT1 complex structure can also perfectly align with the SAH counterpart of the GMS molecule (Fig. 5B). Interestingly, the substrate arginine in the PRMT1 ternary complex is located in a similar position to the guanidino moiety of GMS in the PRMT6 structure (Fig. 5B). Structural comparison of the PRMT6-GMS complex with those of the recently reported other PRMT6 inhibitor complexes revealed that those inhibitors, such as MS023 [34], EPZ0204111 [59] and fragment 7 [35] only occupy the substrate arginine binding pocket, different from the GMS molecule, which occupies both substrate and cofactor binding pockets. Hence, the GMS inhibitor acts as a bi-substrate inhibitor by capturing the interacting features of both the cofactor and the substrate.

Structural basis of asymmetrical dimethylation ability of PRMT6

There are three types of protein arginine methyltransferases, which produce asymmetrical di-methylated, symmetrical di-methylated, and mono-methylated arginine modifications, respectively. But, it is still not very clear how these arginine methyltransferases generate different arginine modification marks. In order to gain insights into the different product specificities of arginine methyltransferases, it is essential to obtain the complex structures of these different types of arginine methyltransferases with their substrates. So far, the substrate complex structures have been reported for the arginine mono-methyltransferase *Trypanosoma brucei* PRMT7 (*Tb*PRMT7) [60, 61], and the human arginine symmetrical di-methyltransferase PRMT5 [54]. Arginine asymmetrical di-methyltransferase PRMT1 has been crystallized with its substrate peptide, and the electron density map revealed just an arginine residue in the substrate binding groove [47]. In this study, we crystallized PRMT6 with its cofactor SAH and a short peptide of GR(me1)G, and obtained a high-resolution crystal structure. From the electron density map, some extra electron density was found near the SAM binding pocket (Supplementary Fig. 2A), and when we superimposed it with the PRMT1-SAH-GR(me1)G ternary complex structure, we found that the side chain of the substrate mono-methyl arginine residue could be fitted into the extra electron density perfectly (Supplementary Fig. 2A). In addition, as we mentioned previously that the guanidino moiety of GMS also resides in the same position as the side chain of the substrate arginine in the PRMT1-SAH-arginine complex structure. Furthermore, during preparation of the manuscript, a CARM1-SNF-peptide complex structure (PDB: 5DWQ) was published, and the target arginine interaction is consistent with what we observed in this study (Supplementary Fig. 3) [62]. Therefore, it is very likely that the extra electron density could

be attributed to the mono-methyl arginine residue of the substrate peptide. Nevertheless, we could not exclude that the extra electron density might arise from some other small molecule, such as the Tris (Tris(hydroxymethyl)aminomethane) buffer molecule (Supplementary Fig. 2B), which we used in our purification buffer.

Interestingly, the putative PRMT6 ternary complex could provide us with insights into how different arginine methylation products are generated. In the PRMT6-SAH-GR(me1)G ternary complex structure (Fig. 5C), the mono-methyl arginine residue forms a salt bridge with the highly conserved E155, and this interaction is also found in the *Tb*PRMT7-SAH-H4R3 peptide complex structure (Fig. 5E, PDB: 4M38) [60] and the PRMT5-SAH-H4R3 peptide complex structure (Fig. 5F, PDB: 4GQB) [54]. The other glutamic acid residue E164 in the double-E loop in both of our PRMT6 structures presented here points away from the substrate arginine, but in a recently reported PRMT6 structure in complex with SAH and an inhibitor EPZ0204111, E164 points towards the inhibitor although it does not form a hydrogen bond with the inhibitor (Fig. 5D, PDB: 4Y30) [59]. When we superimposed E164 from the PRMT6-SAH-EPZ0204111 structure into our PRMT6-SAH-GR(me1)G complex, it could also form a hydrogen bond with the substrate arginine (Fig. 5D). The glutamic acid residue corresponding to E164 of PRMT6 could also form one or two hydrogen bond-mediated salt bridges with the target arginine residue in the *Tb*PRMT7 and PRMT5 complex structures, respectively (Fig. 5E and 5F). Therefore, the two glutamic acid residues in the double-E loop are engaged in the substrate target arginine recognition in all types of arginine methyltransferases.

The two glutamic acid residues in the double-E loop have been found to be critical for methyl transfer activity in different PRMTs [47, 48, 51, 63]. In both CARM1 and PRMT3 structures, the side chains of these two highly conserved glutamic acid residues point towards the pocket, and were proposed to deprotonate the target arginine residue for nucleophilic attack on the methyl donor SAM. In our PRMT6 complex structures, the side chain of E155 points to the arginine binding pocket, but the side chain of the other glutamic acid E164 points away from the pocket (Fig. 5B). The same conformation is observed in the rat PRMT1 structure [47]. The rat PRMT1 was crystallized at a low pH (~4.7), and the protein is inactive under that condition [47]. However, the corresponding glutamic acid in the yeast PRMT1 homolog also adopts the same conformation even when it was crystallized at a high pH (7.5) [46]. In addition, all the PRMT6 structures reported in this study were crystallized at around pH 7.5, which has the optimal enzymatic activity (Supplementary Fig. 4). On the other hand, in the PRMT6 structure in complex with SAH and an inhibitor EPZ0204111, E164 points to the substrate arginine-binding pocket (Fig. 5D, PDB: 4Y30). We then examined all the available structures of PRMT5 and PRMT7 in the PDB database, and found that in all of these available structures, both glutamic acid residues in the double-E loop for these type II and III enzymes always point towards the arginine-binding pocket regardless of the substrate presence in the crystal structures [54, 60, 64, 65]. Taken together, the second glutamic acid in the double-E loop (E164 in the case of PRMT6) is very dynamic in the type I PRMT proteins, and the dynamic nature may be important for catalysis [51].

The substrate mono-methyl arginine in the PRMT6-SAH-GR(me1)G complex structure also forms a hydrogen bond with the side chain of H317 in the PRMT6 structure (Fig. 5C). This

histidine residue is conserved in all the other type I arginine methyltransferases, which corresponds to a glutamine residue in both human and *Trypanosoma brucei* PRMT7 (Q329 in *Tb*PRMT7) (Fig. 2). In the *Tb*PRMT7-SAH-H4R3 ternary structure, Q329 also forms a hydrogen bond with the terminal guanidino nitrogen (Fig. 5E). However, this hydrogen bond is absent in the type II arginine methyltransferase PRMT5, in which the corresponding residue S578 is far away from the substrate arginine (Fig. 5F). Based on the available structural information and previous catalytic studies revealing that arginine di-methylation is processive [66–68], possible methylation mechanisms could be proposed for these different types of arginine methyltransferases. All the arginine methyltransferases utilize the two glutamic acid residues in the double-E loop to deprotonate the Nη1 atom of the target arginine residue, which leads to a methyl group transfer to the Nη1 atom (Fig. 2, 5C, 5E and 5F). Once the first methyl group is transferred, for PRMT7, due to its limited space around the Nη1 atom, an additional methyl group cannot be added to the Nη1 atom to produce asymmetrical di-methylation (Fig. 5E) [60]. The importance of this limited space in determining the product specificity was confirmed by a recent study, in which a point mutation E181D in *Tb*PTMT7, which creates an enlarging space around the Nη1 atom, converts *Tb*PTMT7 from a type III PRMT to a type I PRMT [61]. On the other hand, the hydrogen bond interactions between Q329 or E172, and Nη2 of the substrate arginine would deter methyl-Nη1 and Nη2 from swapping positions because methyl-Nη1 would cause steric clashes with Q329 and E172 when it swaps positions with Nη2 (Fig. 5E). That explains why the type III arginine methyltransferases can only carry out mono-methylation. For the type II arginine methyltransferases, based on the PRMT5-substrate complex structure, S578 does not contact the substrate arginine. This setting would create enough room to accommodate an extra methyl group on the Nη2 side (Fig. 5F). Therefore, once a methyl group is attached to the Nη1 atom, because the second glutamic acid in the double-E loop forms double hydrogen bonds with the substrate arginine, which limits this nitrogen atom to take the second methyl group, the methyl-Nη1 would then rotate to swap positions with Nη2, and Nη2 would be deprotonated again to accept another methyl group to form symmetrical dimethylation. This rotation is necessary because Nη2 is far from the reactive methyl group of the methyl donor SAM to accept the methyl transfer directly (Fig. 5E). For the type I arginine methyltransferases, because the second glutamic acid is very dynamic (Fig. 5C and 5D), it should take a different conformation once it aids the first glutamic acid to deprotonate the target arginine; therefore, two methyl groups could be transferred to the Nη1 atom to form asymmetrical di-methylation.

Because the type I specific histidine residue (H317 in PRMT6) is a critical structural determinant in the asymmetrical di-methylation ability of the type I arginine methyltransferases, mutating it to a type II specific serine residue could potentially alter its product specificity. We, therefore, made a H317S PRMT6 mutant. Our enzymatic assay results revealed that H317S mutant only displayed a slightly reduced activity, but it could not produce any detectable symmetrical di-methylation (Fig. 6A). Structural comparison of the PRMT6, PRMT5 and *Tb*PRMT7 substrate complexes revealed that the type I specific histidine residue (H317 in PRMT6), the type II specific serine residue (S578 in PRMT5) and the type III specific glutamine (Q329 in *Tb*PRMT7) are located in a structural motif, which is highly conserved in their own subfamily, but diverse among these different types of

arginine methyltransferases (Fig. 2 and Fig. 6B). The serine residue (S578 in PRMT5) is significantly farther to the substrate arginine residue than its corresponding residues in type I and III arginine methyltransferases, which would create big enough room to accommodate a methyl group (Fig. 6B). Therefore, the structural element harboring the type-specific residue (H317 in PRMT6) as a whole is the structural determinant in conferring the arginine methylation product specificity of different types of arginine methyltransferases.

Supplementary Material

Refer to Web version on PubMed Central for supplementary material.

Acknowledgments

We thank Dr. Yanli Liu for the critical reading and editing of this manuscript. The SGC is a registered charity (number 1097737) that receives funds from AbbVie, Bayer Pharma AG, Boehringer Ingelheim, Canada Foundation for Innovation, Eshelman Institute for Innovation, Genome Canada through Ontario Genomics Institute, Innovative Medicines Initiative (EU/EFPIA) [ULTRA-DD grant no. 115766], Janssen, Merck & Co., Novartis Pharma AG, Ontario Ministry of Economic Development and Innovation, Pfizer, São Paulo Research Foundation-FAPESP, Takeda, and the Wellcome Trust. Some diffraction experiments were performed at Structural Biology Center and Northeastern Collaborative Access Team beam lines at the Advanced Photon Source, Argonne National Laboratory (ANL). ANL is operated by UChicago Argonne, LLC, for the U.S. Department of Energy, Office of Biological and Environmental Research under contract DE-AC02-06CH11357. The authors are grateful for the financial support from the National Institute of General Medical Science (R01GM096056) and NCI Cancer Center Support Grant (P30 CA08748), the Starr Cancer Consortium, and Mr. William H. Goodwin and Mrs. Alice Goodwin, The Commonwealth Foundation for Cancer Research and The Experimental Therapeutics Center of Memorial Sloan Kettering Cancer Center.

References

1. Boffa LC, Karn J, Vidali G, Allfrey VG. Distribution of NG, NG,-dimethylarginine in nuclear protein fractions. Biochem Biophys Res Commun. 1977; 74:969–976. [PubMed: 843361]
2. Lott K, Li J, Fisk JC, Wang H, Aletta JM, Qu J, Read LK. Global proteomic analysis in trypanosomes reveals unique proteins and conserved cellular processes impacted by arginine methylation. Journal of proteomics. 2013; 91C:210–225.
3. Yang Y, Bedford MT. Protein arginine methyltransferases and cancer. Nature reviews. Cancer. 2013; 13:37–50. [PubMed: 23235912]
4. Yang Y, Hadjikyriacou A, Xia Z, Gayatri S, Kim D, Zurita-Lopez C, Kelly R, Guo A, Li W, Clarke SG, Bedford MT. PRMT9 is a type II methyltransferase that methylates the splicing factor SAP145. Nat Commun. 2015; 6:6428. [PubMed: 25737013]
5. Bedford MT, Clarke SG. Protein arginine methylation in mammals: who, what, and why. Mol Cell. 2009; 33:1–13. [PubMed: 19150423]
6. Friesen WJ, Massenet S, Paushkin S, Wyce A, Dreyfuss G. SMN, the product of the spinal muscular atrophy gene, binds preferentially to dimethylarginine-containing protein targets. Mol Cell. 2001; 7:1111–1117. [PubMed: 11389857]
7. Tripsianes K, Madl T, Machyna M, Fessas D, Englbrecht C, Fischer U, Neugebauer KM, Sattler M. Structural basis for dimethylarginine recognition by the Tudor domains of human SMN and SPF30 proteins. Nat Struct Mol Biol. 2011; 18:1414–1420. [PubMed: 22101937]
8. Liu K, Guo Y, Liu H, Bian C, Lam R, Liu Y, Mackenzie F, Rojas LA, Reinberg D, Bedford MT, Xu RM, Min J. Crystal Structure of TDRD3 and Methyl-Arginine Binding Characterization of TDRD3, SMN and SPF30. PLoS One. 2012; 7:e30375. [PubMed: 22363433]
9. Yong J, Wan L, Dreyfuss G. Why do cells need an assembly machine for RNA-protein complexes? Trends in cell biology. 2004; 14:226–232. [PubMed: 15130578]
10. Liu K, Chen C, Guo Y, Lam R, Bian C, Xu C, Zhao DY, Jin J, Mackenzie F, Pawson T, Min J. Structural basis for recognition of arginine methylated Piwi proteins by the extended Tudor domain. Proc Natl Acad Sci U S A. 2010; 107:18398–18403. [PubMed: 20937909]

11. Chen C, Nott TJ, Jin J, Pawson T. Deciphering arginine methylation: Tudor tells the tale. Nat Rev Mol Cell Biol. 2011; 12:629–642. [PubMed: 21915143]
12. Liu H, Wang JY, Huang Y, Li Z, Gong W, Lehmann R, Xu RM. Structural basis for methylarginine-dependent recognition of Aubergine by Tudor. Genes Dev. 2010
13. Chen C, Jin J, James DA, Adams-Cioaba MA, Park JG, Guo Y, Tenaglia E, Xu C, Gish G, Min J, Pawson T. Mouse Piwi interactome identifies binding mechanism of Tdrkh Tudor domain to arginine methylated Miwi. Proc Natl Acad Sci U S A. 2009; 106:20336–20341. [PubMed: 19918066]
14. Yang Y, Lu Y, Espejo A, Wu J, Xu W, Liang S, Bedford MT. TDRD3 is an effector molecule for arginine-methylated histone marks. Mol Cell. 2010; 40:1016–1023. [PubMed: 21172665]
15. Guccione E, Bassi C, Casadio F, Martinato F, Cesaroni M, Schuchlautz H, Luscher B, Amati B. Methylation of histone H3R2 by PRMT6 and H3K4 by an MLL complex are mutually exclusive. Nature. 2007; 449:933–937. [PubMed: 17898714]
16. Hyllus D, Stein C, Schnabel K, Schiltz E, Imhof A, Dou Y, Hsieh J, Bauer UM. PRMT6-mediated methylation of R2 in histone H3 antagonizes H3 K4 trimethylation. Genes Dev. 2007; 21:3369–3380. [PubMed: 18079182]
17. Kirmizis A, Santos-Rosa H, Penkett CJ, Singer MA, Vermeulen M, Mann M, Bahler J, Green RD, Kouzarides T. Arginine methylation at histone H3R2 controls deposition of H3K4 trimethylation. Nature. 2007; 449:928–932. [PubMed: 17898715]
18. Iberg AN, Espejo A, Cheng D, Kim D, Michaud-Levesque J, Richard S, Bedford MT. Arginine methylation of the histone H3 tail impedes effector binding. The Journal of biological chemistry. 2008; 283:3006–3010. [PubMed: 18077460]
19. Migliori V, Muller J, Phalke S, Low D, Bezzi M, Mok WC, Sahu SK, Gunaratne J, Capasso P, Bassi C, Cecatiello V, De Marco A, Blackstock W, Kuznetsov V, Amati B, Mapelli M, Guccione E. Symmetric dimethylation of H3R2 is a newly identified histone mark that supports euchromatin maintenance. Nat Struct Mol Biol. 2012; 19:136–144. [PubMed: 22231400]
20. Qin S, Liu Y, Tempel W, Eram MS, Bian C, Liu K, Senisterra G, Crombet L, Vedadi M, Min J. Structural basis for histone mimicry and hijacking of host proteins by influenza virus protein NS1. Nat Commun. 2014; 5:3952. [PubMed: 24853335]
21. Schuetz A, Allali-Hassani A, Martin F, Loppnau P, Vedadi M, Bochkarev A, Plotnikov AN, Arrowsmith CH, Min J. Structural basis for molecular recognition and presentation of histone H3 by WDR5. Embo J. 2006; 25:4245–4252. [PubMed: 16946699]
22. Patel A, Dharmarajan V, Cosgrove MS. Structure of WDR5 bound to mixed lineage leukemia protein-1 peptide. J Biol Chem. 2008; 283:32158–32161. [PubMed: 18829459]
23. Dharmarajan V, Lee JH, Patel A, Skalnik DG, Cosgrove MS. Structural basis for WDR5 interaction (Win) motif recognition in human SET1 family histone methyltransferases. J Biol Chem. 2012; 287:27275–27289. [PubMed: 22665483]
24. Zhang P, Lee H, Brunzelle JS, Couture JF. The plasticity of WDR5 peptide-binding cleft enables the binding of the SET1 family of histone methyltransferases. Nucleic acids research. 2012; 40:4237–4246. [PubMed: 22266653]
25. Yoshimatsu M, Toyokawa G, Hayami S, Unoki M, Tsunoda T, Field HI, Kelly JD, Neal DE, Maehara Y, Ponder BA, Nakamura Y, Hamamoto R. Dysregulation of PRMT1 and PRMT6, Type I arginine methyltransferases, is involved in various types of human cancers. International journal of cancer. Journal international du cancer. 2011; 128:562–573. [PubMed: 20473859]
26. Kleinschmidt MA, de Graaf P, van Teeffelen HA, Timmers HT. Cell cycle regulation by the PRMT6 arginine methyltransferase through repression of cyclin-dependent kinase inhibitors. PLoS One. 2012; 7:e41446. [PubMed: 22916108]
27. Phalke S, Mzoughi S, Bezzi M, Jennifer N, Mok WC, Low DH, Thike AA, Kuznetsov VA, Tan PH, Voorhoeve PM, Guccione E. p53-Independent regulation of p21Waf1/Cip1 expression and senescence by PRMT6. Nucleic acids research. 2012; 40:9534–9542. [PubMed: 22987071]
28. Stein C, Riedl S, Ruthnick D, Notzold RR, Bauer UM. The arginine methyltransferase PRMT6 regulates cell proliferation and senescence through transcriptional repression of tumor suppressor genes. Nucleic acids research. 2012; 40:9522–9533. [PubMed: 22904088]

29. Michaud-Levesque J, Richard S. Thrombospondin-1 is a transcriptional repression target of PRMT6. J Biol Chem. 2009; 284:21338–21346. [PubMed: 19509293]
30. Kim NH, Kim SN, Seo DW, Han JW, Kim YK. PRMT6 overexpression upregulates TSP-1 and downregulates MMPs: its implication in motility and invasion. Biochem Biophys Res Commun. 2013; 432:60–65. [PubMed: 23380452]
31. Herglotz J, Kuvardina ON, Kolodziej S, Kumar A, Hussong H, Grez M, Lausen J. Histone arginine methylation keeps RUNX1 target genes in an intermediate state. Oncogene. 2013; 32:2565–2575. [PubMed: 22777353]
32. Lee YH, Ma H, Tan TZ, Ng SS, Soong R, Mori S, Fu XY, Zernicka-Goetz M, Wu Q. Protein arginine methyltransferase 6 regulates embryonic stem cell identity. Stem cells and development. 2012; 21:2613–2622. [PubMed: 22455726]
33. Boulanger MC, Liang C, Russell RS, Lin R, Bedford MT, Wainberg MA, Richard S. Methylation of Tat by PRMT6 regulates human immunodeficiency virus type 1 gene expression. Journal of virology. 2005; 79:124–131. [PubMed: 15596808]
34. Eram MS, Shen Y, Szewczyk MM, Wu H, Senisterra G, Li F, Butler KV, Kaniskan HU, Speed BA, dela Sena C, Dong A, Zeng H, Schapira M, Brown PJ, Arrowsmith CH, Barsyte-Lovejoy D, Liu J, Vedadi M, Jin J. A Potent, Selective, and Cell-Active Inhibitor of Human Type I Protein Arginine Methyltransferases. ACS chemical biology. 2016; 11:772–781. [PubMed: 26598975]
35. Ferreira de Freitas R, Eram MS, Szewczyk MM, Steuber H, Smil D, Wu H, Li F, Senisterra G, Dong A, Brown PJ, Hitchcock M, Moosmayer D, Stegmann CM, Egner U, Arrowsmith C, Barsyte-Lovejoy D, Vedadi M, Schapira M. Discovery of a Potent Class I Protein Arginine Methyltransferase Fragment Inhibitor. Journal of medicinal chemistry. 2016; 59:1176–1183. [PubMed: 26824386]
36. Eram MS, Bustos SP, Lima-Fernandes E, Siarheyeva A, Senisterra G, Hajian T, Chau I, Duan S, Wu H, Dombrovski L, Schapira M, Arrowsmith CH, Vedadi M. Trimethylation of histone H3 lysine 36 by human methyltransferase PRDM9 protein. The Journal of biological chemistry. 2014; 289:12177–12188. [PubMed: 24634223]
37. Barsyte-Lovejoy D, Li F, Oudhoff MJ, Tatlock JH, Dong A, Zeng H, Wu H, Freeman SA, Schapira M, Senisterra GA, Kuznetsova E, Marcellus R, Allali-Hassani A, Kennedy S, Lambert JP, Couzens AL, Aman A, Gingras AC, Al-Awar R, Fish PV, Gerstenberger BS, Roberts L, Benn CL, Grimley RL, Braam MJ, Rossi FM, Sudol M, Brown PJ, Bunnage ME, Owen DR, Zaph C, Vedadi M, Arrowsmith CH. (R)-PFI-2 is a potent and selective inhibitor of SETD7 methyltransferase activity in cells. Proceedings of the National Academy of Sciences of the United States of America. 2014; 111:12853–12858. [PubMed: 25136132]
38. Lakowski TM, Szeitz A, Pak ML, Thomas D, Vhuiyan MI, Kotthaus J, Clement B, Frankel A. MS(3) fragmentation patterns of monomethylarginine species and the quantification of all methylarginine species in yeast using MRM(3). Journal of proteomics. 2013; 80:43–54. [PubMed: 23333926]
39. Otwinowski ZMW. Processing of X-ray diffraction data collected in oscillation mode. Meth Enzymol. 1997; 276:307–326.
40. Vagin ATA. MOLREP: an Automated Program for Molecular Replacement. J Appl Cryst. 1997; 30:1022–1025.
41. Murshudov GN, Vagin AA, Dodson EJ. Refinement of macromolecular structures by the maximum-likelihood method. Acta Crystallogr D Biol Crystallogr. 1997; 53:240–255. [PubMed: 15299926]
42. Emsley P, Cowtan K. Coot: Model-building tools for molecular graphics. Acta Crystallographica. 2004; D60:2126–2132.
43. Davis IW, Murray LW, Richardson JS, Richardson DC. MOLPROBITY: structure validation and all-atom contact analysis for nucleic acids and their complexes. Nucleic acids research. 2004; 32:W615–619. [PubMed: 15215462]
44. Lo Sardo A, Altamura S, Pegoraro S, Maurizio E, Sgarra R, Manfioletti G. Identification and characterization of new molecular partners for the protein arginine methyltransferase 6 (PRMT6). PLoS One. 2013; 8:e53750. [PubMed: 23326497]

45. Goulet I, Gauvin G, Boisvenue S, Cote J. Alternative splicing yields protein arginine methyltransferase 1 isoforms with distinct activity, substrate specificity, and subcellular localization. J Biol Chem. 2007; 282:33009–33021. [PubMed: 17848568]

46. Weiss VH, McBride AE, Soriano MA, Filman DJ, Silver PA, Hogle JM. The structure and oligomerization of the yeast arginine methyltransferase, Hmt1. Nat Struct Biol. 2000; 7:1165–1171. [PubMed: 11101900]

47. Zhang X, Cheng X. Structure of the predominant protein arginine methyltransferase PRMT1 and analysis of its binding to substrate peptides. Structure. 2003; 11:509–520. [PubMed: 12737817]

48. Zhang X, Zhou L, Cheng X. Crystal structure of the conserved core of protein arginine methyltransferase PRMT3. EMBO J. 2000; 19:3509–3519. [PubMed: 10899106]

49. Siarheyeva A, Senisterra G, Allali-Hassani A, Dong A, Dobrovetsky E, Wasney GA, Chau I, Marcellus R, Hajian T, Liu F, Korboukh I, Smil D, Bolshan Y, Min J, Wu H, Zeng H, Loppnau P, Poda G, Griffin C, Aman A, Brown PJ, Jin J, Al-Awar R, Arrowsmith CH, Schapira M, Vedadi M. An allosteric inhibitor of protein arginine methyltransferase 3. Structure. 2012; 20:1425–1435. [PubMed: 22795084]

50. Troffer-Charlier N, Cura V, Hassenboehler P, Moras D, Cavarelli J. Functional insights from structures of coactivator-associated arginine methyltransferase 1 domains. EMBO J. 2007; 26:4391–4401. [PubMed: 17882262]

51. Yue WW, Hassler M, Roe SM, Thompson-Vale V, Pearl LH. Insights into histone code syntax from structural and biochemical studies of CARM1 methyltransferase. EMBO J. 2007; 26:4402–4412. [PubMed: 17882261]

52. Bonnefond L, Stojko J, Mailliot J, Troffer-Charlier N, Cura V, Wurtz JM, Cianferani S, Cavarelli J. Functional insights from high resolution structures of mouse protein arginine methyltransferase 6. Journal of structural biology. 2015; 191:175–183. [PubMed: 26094878]

53. Wang C, Zhu Y, Chen J, Li X, Peng J, Chen J, Zou Y, Zhang Z, Jin H, Yang P, Wu J, Niu L, Gong Q, Teng M, Shi Y. Crystal structure of arginine methyltransferase 6 from Trypanosoma brucei. PloS one. 2014; 9:e87267. [PubMed: 24498306]

54. Antonysamy S, Bonday Z, Campbell RM, Doyle B, Druzina Z, Gheyi T, Han B, Jungheim LN, Qian Y, Rauch C, Russell M, Sauder JM, Wasserman SR, Weichert K, Willard FS, Zhang A, Emtage S. Crystal structure of the human PRMT5:MEP50 complex. Proceedings of the National Academy of Sciences of the United States of America. 2012; 109:17960–17965. [PubMed: 23071334]

55. Ghosh AK, Liu W. Total Synthesis of (+)-Sinefungin. J Org Chem. 1996; 61:6175–6182. [PubMed: 11667452]

56. Zheng W, Ibanez G, Wu H, Blum G, Zeng H, Dong A, Li F, Hajian T, Allali-Hassani A, Amaya MF, Siarheyeva A, Yu W, Brown PJ, Schapira M, Vedadi M, Min J, Luo M. Sinefungin Derivatives as Inhibitors and Structure Probes of Protein Lysine Methyltransferase SETD2. J Am Chem Soc. 2012; 134:18004–18014. [PubMed: 23043551]

57. Maria EJ, Da SAD, Fourrey J-L. A radical-based strategy for the synthesis of higher homologues of sinefungin. Eur J Org Chem. 2000:627–631.

58. Bailey PD, Beard MA, Dang HPT, Phillips TR, Price RA, Whittaker JH. Debenzylation using catalytic hydrogenolysis in trifluoroethanol, and the total synthesis of (-)-raumacline. Tetrahedron Lett. 2008; 49:2150–2153.

59. Mitchell LH, Drew AE, Ribich SA, Rioux N, Swinger KK, Jacques SL, Lingaraj T, Boriack-Sjodin PA, Waters NJ, Wigle TJ, Moradei O, Jin L, Riera T, Porter-Scott M, Moyer MP, Smith JJ, Chesworth R, Copeland RA. Aryl Pyrazoles as Potent Inhibitors of Arginine Methyltransferases: Identification of the First PRMT6 Tool Compound. ACS medicinal chemistry letters. 2015; 6:655–659. [PubMed: 26101569]

60. Wang C, Zhu Y, Caceres TB, Liu L, Peng J, Wang J, Chen J, Chen X, Zhang Z, Zuo X, Gong Q, Teng M, Hevel JM, Wu J, Shi Y. Structural determinants for the strict monomethylation activity by trypanosoma brucei protein arginine methyltransferase 7. Structure. 2014; 22:756–768. [PubMed: 24726341]

61. Debler EW, Jain K, Warmack RA, Feng Y, Clarke SG, Blobel G, Stavropoulos P. A glutamate/aspartate switch controls product specificity in a protein arginine methyltransferase. Proceedings

of the National Academy of Sciences of the United States of America. 2016; 113:2068–2073. [PubMed: 26858449]

62. Boriack-Sjodin PA, Jin L, Jacques SL, Drew A, Sneeringer C, Scott MP, Moyer MP, Ribich S, Moradei O, Copeland RA. Structural Insights into Ternary Complex Formation of Human CARM1 with Various Substrates. ACS chemical biology. 2015
63. Lee YH, Koh SS, Zhang X, Cheng X, Stallcup MR. Synergy among nuclear receptor coactivators: selective requirement for protein methyltransferase and acetyltransferase activities. Mol Cell Biol. 2002; 22:3621–3632. [PubMed: 11997499]
64. Ho MC, Wilczek C, Bonanno JB, Xing L, Seznec J, Matsui T, Carter LG, Onikubo T, Kumar PR, Chan MK, Brenowitz M, Cheng RH, Reimer U, Almo SC, Shechter D. Structure of the arginine methyltransferase PRMT5-MEP50 reveals a mechanism for substrate specificity. PLoS One. 2013; 8:e57008. [PubMed: 23451136]
65. Sun L, Wang M, Lv Z, Yang N, Liu Y, Bao S, Gong W, Xu RM. Structural insights into protein arginine symmetric dimethylation by PRMT5. Proc Natl Acad Sci U S A. 2011; 108:20538–20543. [PubMed: 22143770]
66. Lakowski TM, Frankel A. A kinetic study of human protein arginine N-methyltransferase 6 reveals a distributive mechanism. The Journal of biological chemistry. 2008; 283:10015–10025. [PubMed: 18263580]
67. Osborne TC, Obianyo O, Zhang X, Cheng X, Thompson PR. Protein arginine methyltransferase 1: positively charged residues in substrate peptides distal to the site of methylation are important for substrate binding and catalysis. Biochemistry. 2007; 46:13370–13381. [PubMed: 17960915]
68. Wang M, Xu RM, Thompson PR. Substrate specificity, processivity, and kinetic mechanism of protein arginine methyltransferase 5. Biochemistry. 2013; 52:5430–5440. [PubMed: 23866019]

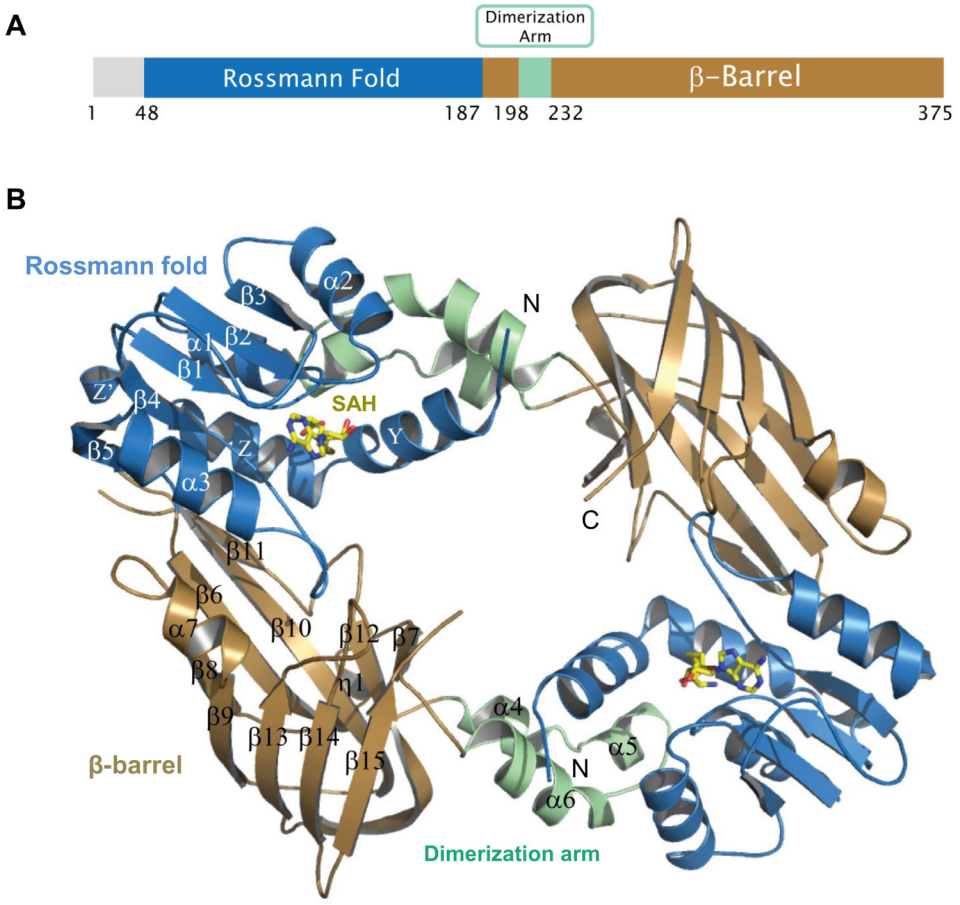

Figure 1.

Crystal structure of the full length human PRMT6 in complex with SAH (PDB: 4HC4, this work). (A) Domain structure of human PRMT6. (B) Overall crystal structure of human PRMT6 in complex with SAH. SAH is shown as a stick model.

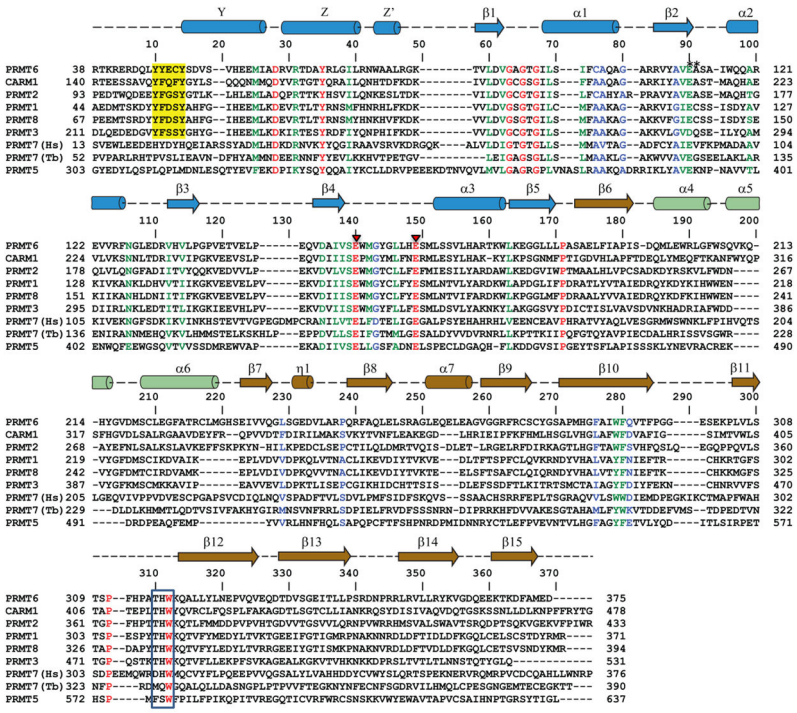

Figure 2.

Sequence alignment of human arginine methyltransferases PRMT1-8 and T*b*PRMT7. The secondary structure elements of PRMT6 are shown on top of the sequence alignment, with cylinder representing α helixes and arrows representing β strands. The identical residues are colored in red, very similar in green, similar in blue and the rest are in black. Red triangles denote the two glutamic acid residues in the double-E loop interacting with the substrate arginine. The N-terminal conserved Y(F/Y)xxY motif found in Type I PRMTs are highlighted in yellow, and the C-terminal THW motif is boxed.

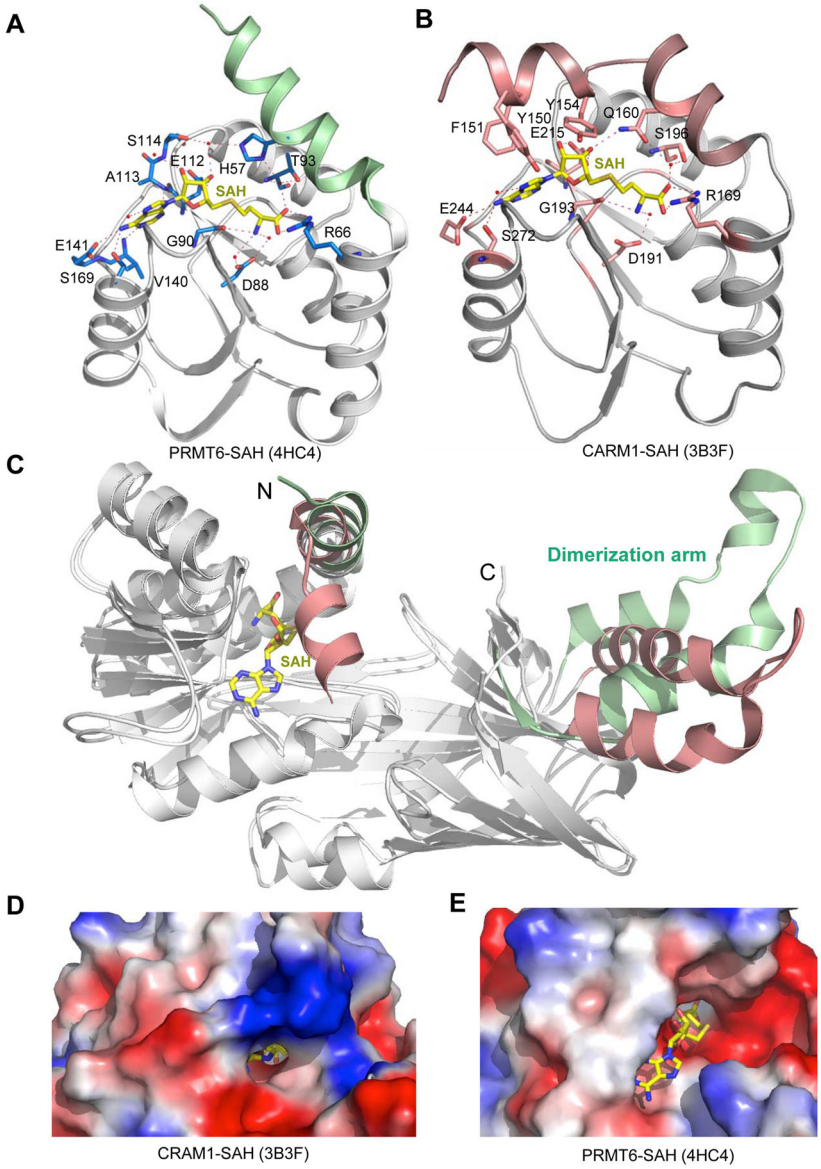

Figure 3.

Structural comparison of PRMT6 (PDB: 4HC4, this work) and CARM1 (PDB: 3B3F). (A) Detailed interactions between PRMT6 and SAH. (B) Detailed interactions between CARM1 and SAH. SAH is shown in a stick model in yellow. Residues contributing to SAH interactions from PRMT6 and CARM1 are shown in stick models, hydrogen bonds are displayed as dashed lines, and water molecules are shown as red spheres. (C) Superposition of the PRMT6-SAH and CARM1-SAH complex structures. SAH is shown in a stick model in yellow. The N-terminal α-helix and dimerization arm are colored in green (in PRMT6) and pink (in CARM1). (D) Electrostatic surface representation of CARM1. (E) Electrostatic surface representation of PRMT6. SAH is shown in a stick model.

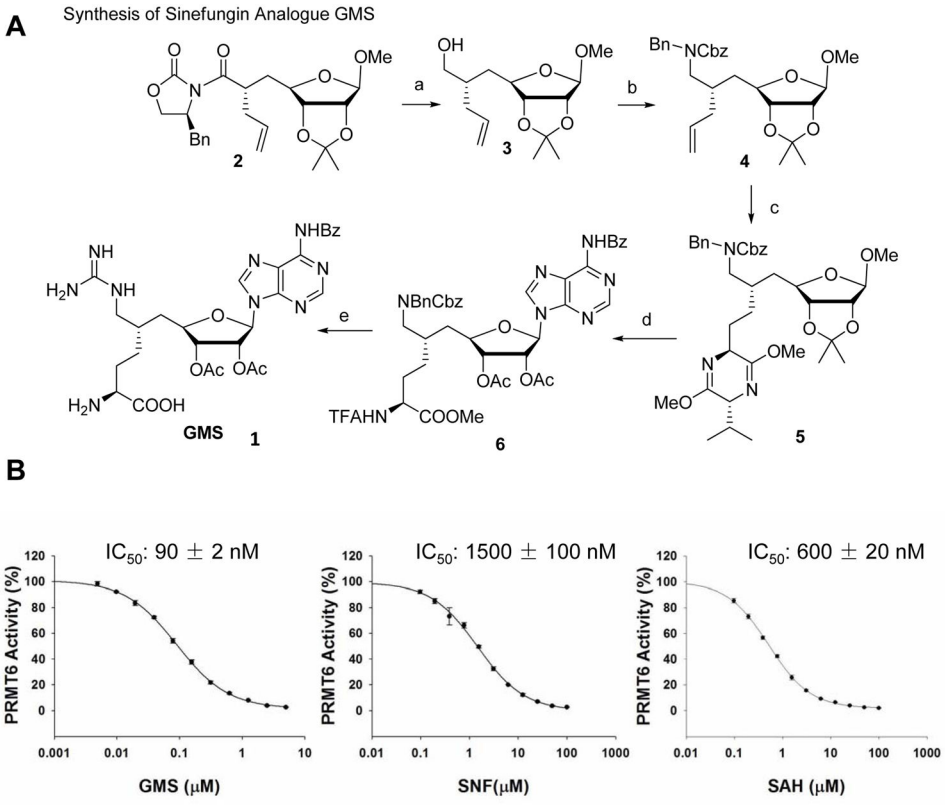

Figure 4.

Development of PRMT6 inhibitor GMS. (A) Synthesis of sinefungin (SNF) analogue GMS. (B) Comparison of the inhibition effect of GMS on PRMT6 with SAH and SNF. The data points were averaged from three independent experiments and were plotted and fitted using the SigmaPlot v11.0. The variation of the values from three experiments is shown as error bars on each data point.

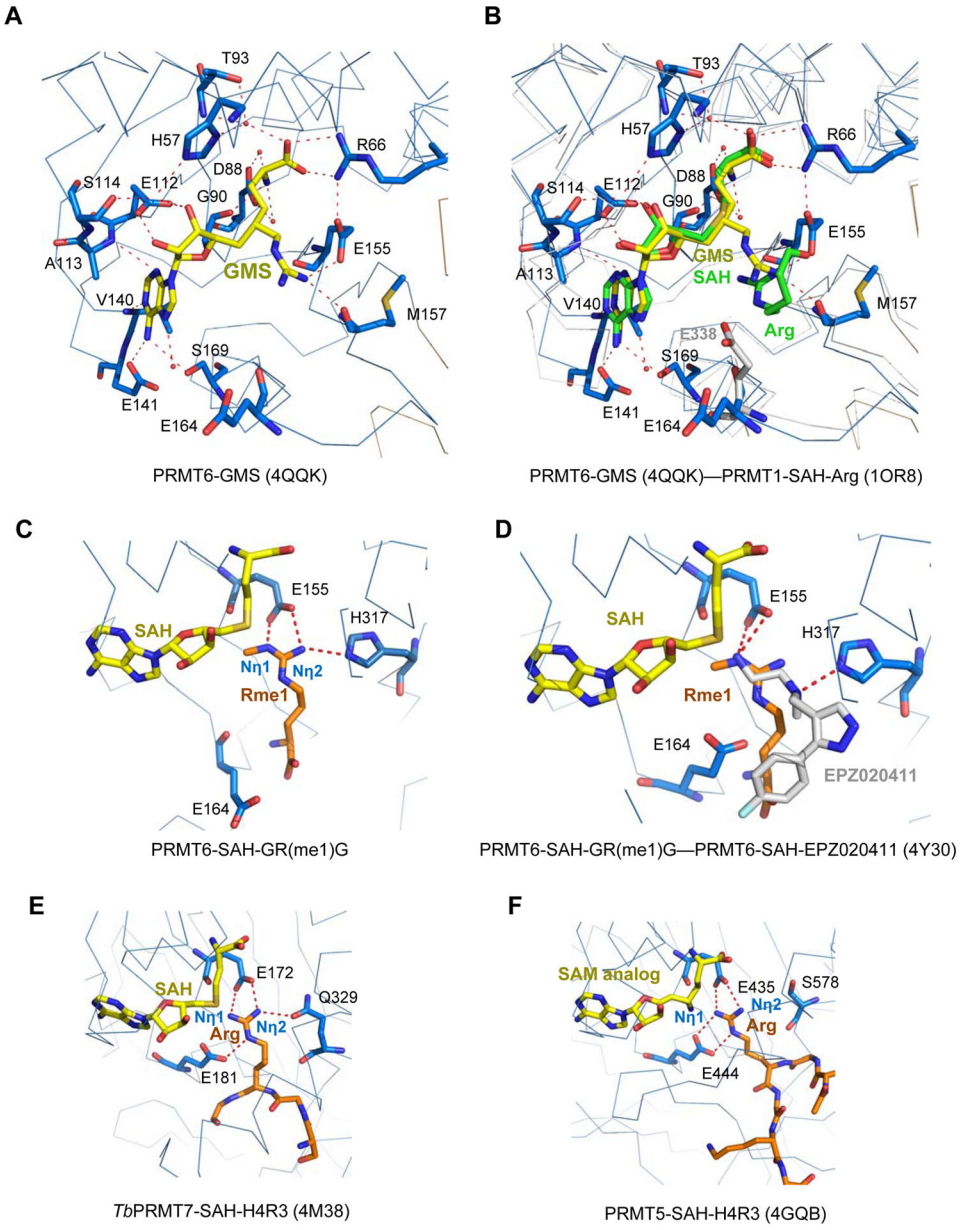

Figure 5.

Structural comparison of arginine methyltransferases in complex with different ligands. (A) Detailed interactions between PRMT6 and the bi-substrate inhibitor GMS (PDB: 4QQK, this work). GMS is shown in a stick model and colored in yellow. The GMS interaction residues in PRMT6 are shown in stick models. (B) Superposition of the PRMT6-GMS (PDB: 4QQK, this work), PRMT1-SAH-arginine (PDB: 1OR8) and PRMT3-SAH (PDB: 2FYT). PRMT6, PRMT1 and PRMT3 have very conserved structures. For clarity, only PRMT6 (blue) and PRMT1 (grey) are shown in ribbons. GMS from the PRMT6 structure is shown in a yellow stick model. SAH and the substrate arginine residue from the PRMT1-SAH-arginine structure are shown in green stick models. For PRMT3 structure, only the second glutamic acid residue E338 from the double-E loop of PRMT3 is shown in a grey

stick model. (C) Detailed interactions between PRMT6 and the mono-methyl arginine of the GR(me1)G peptide. E164 is superimposed from the PRMT6-SAH-EPZ020411 structure. (D) Superposition of the PRMT6-SAH-GR(me1)G and PRMT6-SAH-EPZ020411 (PDB: 4Y30). SAH, mono-methyl arginine, EPZ020411 and the interacting residues in PRMT6 are shown in stick models and colored in yellow, orange, grey, and blue, respectively. (E) Detailed interactions between *Tb*PRMT7 and the substrate arginine residue (PDB: 4M38). (F) Detailed interactions between PRMT5 and the substrate arginine residue (PDB: 4GQB).

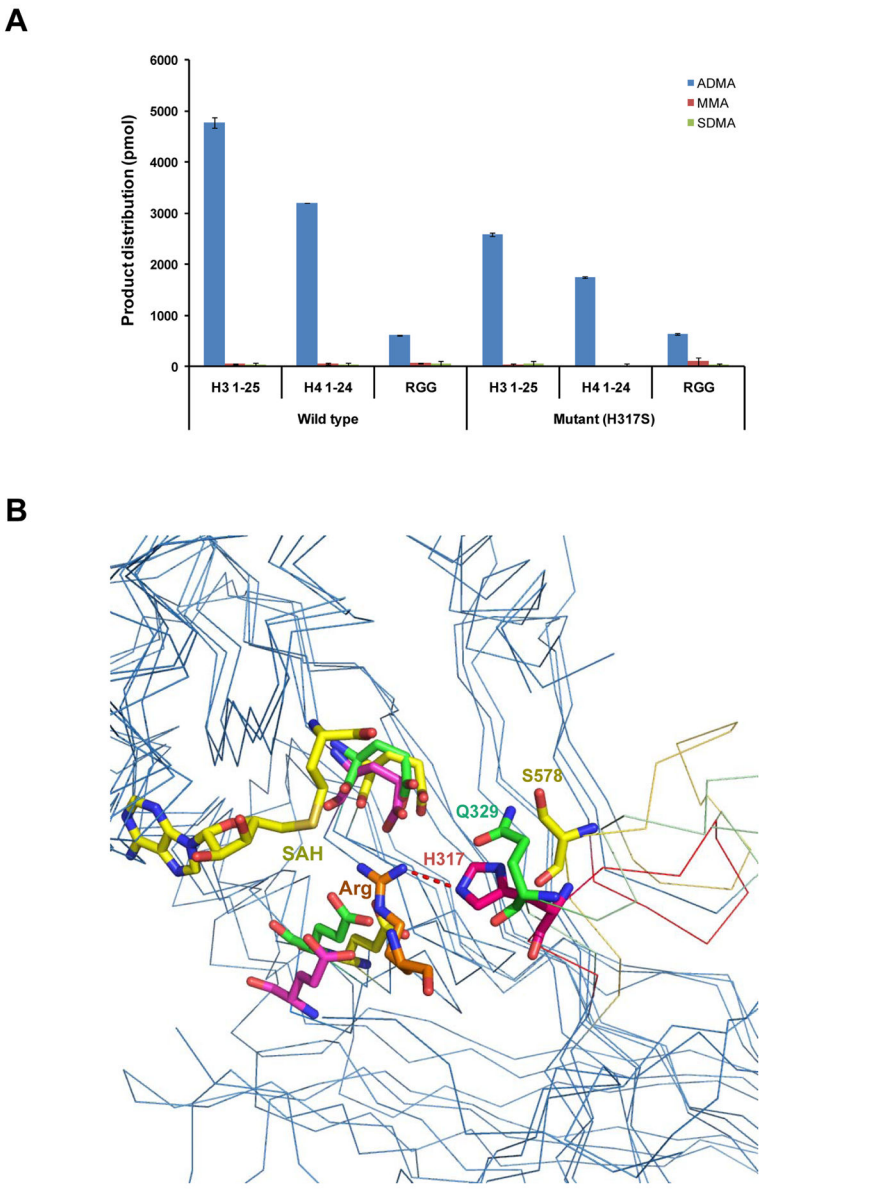

Figure 6.

Structural basis of product specificity for PRMTs. (A) Mutagenesis effect of the type I specific histidine residue in THW motif on product specificity. Mutating H317 to serine in PRMT6 does not change its product specificity significantly. (B) Structural comparison of the substrate binding sites of type I (PRMT6-SAH-GR(me1)G, PDB: 5HZM), II (PRMT5-SAH-H4R3, PDB: 4GQB) and III (*Tb*PRMT7-SAH-H4R3, PDB: 4M38) arginine methyltransferases. All the PRMTs are shown in ribbons. The cofactor SAH, the substrate arginine residue and the type I specific histidine residue in THW motif (H317 of PRMT6) or its corresponding residues in type II/III arginine methyltransferases (S578 of PRMT5 and Q329 of *Tb*PRMT7) are shown in stick models and colored in pink, yellow and green,

respectively. Residues contributing to substrate interactions from PRMT6, PRMT5 and *Tb*PRMT7 are shown in stick models and colored in pink, yellow and green, respectively.

Table 1

Crystallography data and refinement statistics

	PRMT6 + SAH	PRMT6 + GMS	PRMT6+SAH+GR(me1)G
PDB Code	4HC4	4QQK	5HZM
Data collection			
Space group	$I4_1$	$I4_1$	$I4_1$
Cell dimensions			
a, *b*, *c* (Å)	93.98, 93.98, 108.88	95.21,95.21,108.36	94.19,94.19,109,61
α, *β*, *γ* (°)	90, 90, 90	90, 90, 90	90, 90, 90
Resolution (Å) (highest resolution shell)	50.00–1.97(2.00–1.97)	50.00–1.88(1.91–1.88)	50.00–2.02(2.05–2.02)
Measured reflections	332394	326362	232791
Unique reflections	33354	39024	31311
R_{merge}	6.1(74.6)	6.0(70.4)	6.5(98.5)
$I/\sigma I$	42.1(2.8)	38.2(2.8)	36.6(2.3)
Completeness (%)	99.9(100.0)	100.0(100.0)	100.0(100.0)
Redundancy	10.0(10.0)	8.4(8.4)	7.4(7.4)
Refinement			
Resolution (Å)	33.25–1.97	33.79–1.88	50.00–2.02
No. reflections (test set)	33322(1052)	37413(1598)	30302(991)
R_{work}/R_{free} (%)	18.8/22.0	17.7/20.7	17.5/20.5
No. atoms			
Protein	2633	2540	2636
Co-factor	26	31	26
Water	235	193	188
B-factors (Å^2)			
Protein	37.9	32.5	41.4
Compound	34.1	27.4	34.9
Water	47.5	41.0	48.1
RMSD			
Bond lengths (Å)	0.007	0.009	0.011
Bond angles (°)	1.2	1.3	1.4
Ramachandran plot % residues			
Favored	98.2	98.8	98.5
Additional allowed	1.8	1.2	1.5
Generously allowed	0.0	0.0	0.0
Disallowed	0.0	0.0	0.0